

# Correlation of Microstructure with Mechanical Properties of 300M Steel

J. L. YOUNGBLOOD AND M. RAGHAVAN

300M steel was subjected to a wide range of quenched and tempered heat treatments. The plane-strain fracture toughness and the tensile ultimate and yield strengths were evaluated. Results indicate that substantial improvement in toughness with no loss in strength can be accomplished in quenched and tempered steel by austenitizing at 1255 K (1800°F) or higher. Low fracture toughness in conventionally austenitized 300M steel (1144 K (1600°F)) appears to be caused by undissolved precipitates seen both in the sub-microstructure and on the fracture surface which promote failure by quasi-cleavage. These precipitates appeared to dissolve in the range 1200 to 1255 K (1700 to 1800°F).

THE correlation of microstructure with mechanical properties of structural materials has been a topic of interest for many years attracting the attention of numerous workers.<sup>1-21</sup> Most of these studies have been primarily focused either on mechanical properties or on microstructural details, and as a result, many ambiguities and unresolved questions remain. It is believed to be of utmost importance that equal emphasis be placed on both microstructure and mechanical behavior, and the present investigation was undertaken with this dual emphasis as its cornerstone.

300M steel is a widely used ultrahigh strength steel, and considerable research has been conducted into its mechanical properties.<sup>10,22-25</sup> The present research attempts to add to these earlier studies by exploring in depth the influence of conventional quenching and tempering treatments over as wide a temperature range as is practical for steels. The tensile strength and fracture toughness as well as the microstructure and fracture surface morphology were evaluated for each heat treatment.

Explanations are offered as to the mechanisms responsible for the observed mechanical behavior. Heat treatments are also recommended which should give an optimum combination of strength and toughness in practical applications.

## EXPERIMENTAL PROCEDURE

### Materials and Heat Treatment

The 300M steel used in the present study was obtained from Latrobe Steel Company\* and met the

\*Latrobe Steel Company, Latrobe, Pa. 15650.

specifications of AMS-6416. It was vacuum arc melted with a chemical composition given by the manufacturer as 0.41 C, 1.65 Si, 0.65 Mn, 0.002 S, 0.008 P, 0.78 Cr, 0.10 V, 1.77 Ni, 0.42 Mo. About  $2.3 \times 10^5$  g (500 lb) of steel was obtained in two different forms: 1) 0.0762 m  $\times$  0.0127 m (3 in.  $\times$  1/2 in.) section bar stock and 2) 0.0762 m  $\times$  0.0254 m (3 in.  $\times$  1 in.)

J. L. YOUNGBLOOD, formerly Research Metallurgist at NASA-Johnson Space Center, Houston, TX, is now President, Gemini Detectors, Inc., P.O. Box 58746, Houston, TX 77058. M. RAGHAVAN, formerly NRC Postdoctoral Research Associate at NASA-Johnson Space Center, is Engineering Specialist, Olin-Corporation, Metals Research Laboratories, 91 Shelton Ave., New Haven, CT 06504.

Manuscript submitted August 25, 1976.

section bar stock. All material had been normalized at 1183 K (1670°F) for 1 h prior to delivery.

Specimens were austenitized for 1 h in a vertical tube furnace having a uniform heat zone of 0.30 m (12 in.) in a continuously flowing helium atmosphere, directly quenched in oil at room temperature, and double tempered (2 + 2 h) in a salt bath (oil quenched after each tempering treatment). Temperatures employed were as follows:

Austenitizing Temperatures		Tempering Temperatures for Each Austenitizing Temperature	
K	(°F)	K	(°F)
1144	(1600)	Untempered	
1255	(1800)	477	(400)
1366	(2000)	589	(600)
1477	(2200)	700	(800)
		811	(1000)

### Test Specimens and Test Procedures

Compact tension fracture toughness specimens using a crack-opening displacement gage were employed following the procedure outlined in ASTM E399-72 (revised). Specimens were machined from both sizes of bar stock in the long transverse orientation.

Longitudinal tension specimens with square gage sections were machined from the same materials. A 0.025 m (1 in.) extensometer (10 pct strain calibrated) and/or strain gage provided strain during the tests. 0.2 pct offset yield strength and ultimate tensile strength were determined.

### Metallography and Electron Microscopy

Specimens for optical and transmission electron microscopy were obtained from the grip section of the tested tensile specimens. Specimens for transmission electron microscopy were prepared by thinning specimens chemically and jet polishing to perforation.<sup>26</sup> These specimens were examined in a JEM 7 electron microscope using 100 KV potential. Fracture toughness failure surfaces were examined directly in a Cambridge Steroscan S4 scanning electron microscope using 30 KV potential. High resolution fracture surfaces were prepared by coating them with about 300Å of gold and observed using 20 KV potential.

## RESULTS

### Mechanical Properties

**Quenched and Tempered Steels.** Figures 1 to 3 show the effect of tempering on the strength and toughness of the steel. Plain strain fracture toughness,  $K_{IC}$  and the ultimate strength were observed to be independent of thickness over the size range tested so that Figs. 1 and 3 represent the response of both sample groups. Normally only one data point was taken for each heat treatment. Numerical data from which these curves were derived have been presented elsewhere.<sup>27</sup> One can readily see from Fig. 1 that it is possible to separate the specimens into two groups based on the tempering response of the steel. For convenience, specimens quenched from 1144 K (1600°F) will be referred to as Class A specimens and all those quenched from higher temperatures will be referred to as Class B specimens. The curves indicate the following: fracture toughness of the Class A specimens increases almost monotonically with tempering temperature, this increase being

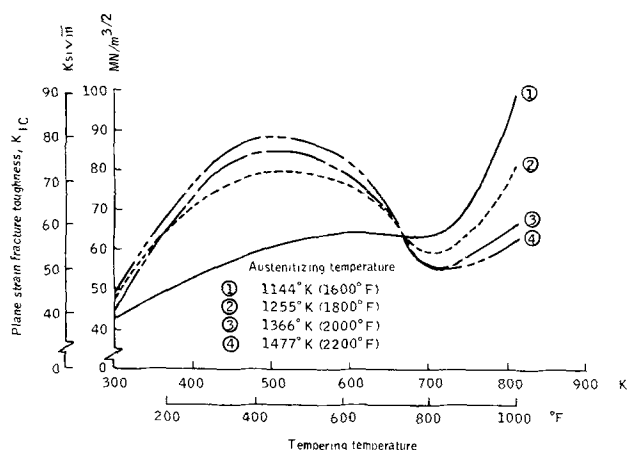


Fig. 1—Effect of tempering temperature on the plane-strain fracture toughness of 300M steel; long transverse orientation; single data points for each thickness.

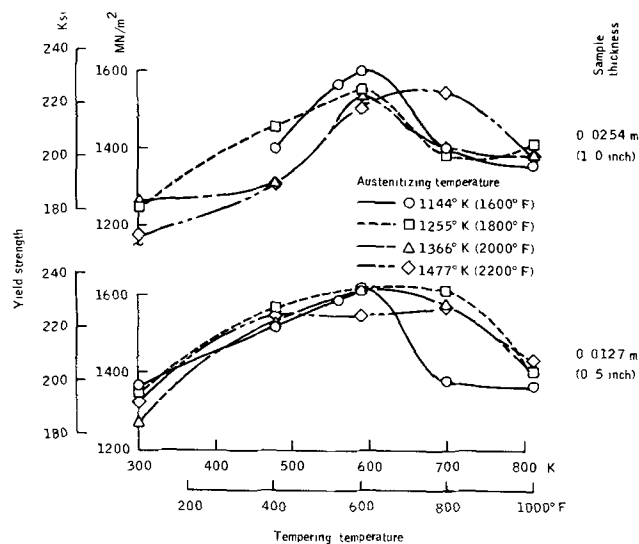


Fig. 2—Effect of tempering temperature on the 0.2 pct tensile yield strength of 300M steel; single data points as shown.

very gradual below 700 K (800°F). In contrast, fracture toughness of the Class B specimens increases rapidly with tempering temperature up to 589 K (600°F) but then declines sharply reaching a minimum in toughness at about 700 K (800°F) and finally increases again with higher tempering temperature up to 811 K (1000°F). No parallel differences between these two classes of specimens were observed in the tensile properties shown in Figs. 2 and 3.

Effect of austenitizing temperature on the fracture toughness of the steel for selected tempering temperatures is shown in Fig. 4. Fracture toughness of as-quenched specimens and specimens tempered at 700 K (800°F) were relatively unaffected by austenitizing temperature. Toughness of the specimens tempered at 477 K (400°F) and 589 K (600°F) increased with austenitizing temperature while tempering at 811 K (1000°F) showed a decrease in toughness with increasing austenitizing temperature. This suggests that the effects of austenitizing temperature and tempering temperature on toughness are interrelated.

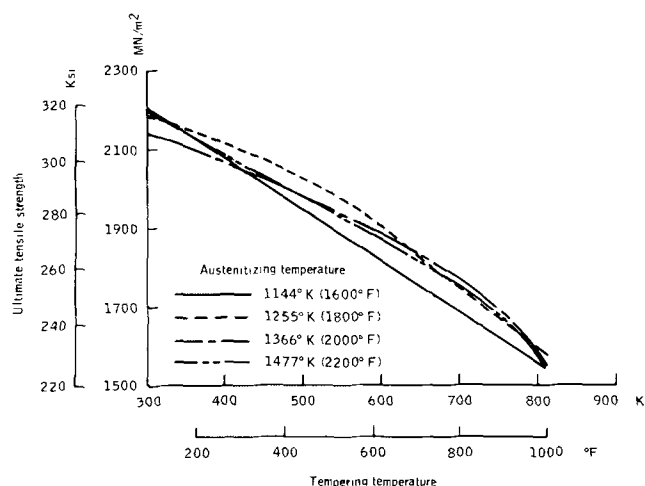


Fig. 3—Effect of tempering and austenitizing temperatures on the ultimate tensile strength of 300M steel; single data points for each thickness.

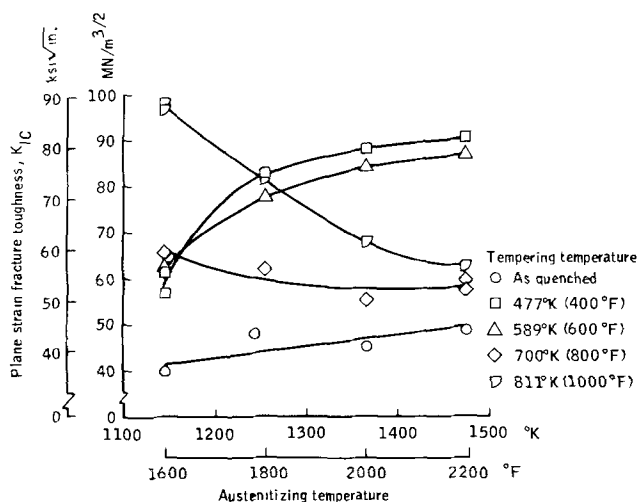


Fig. 4—Effect of austenitizing temperature on the plane strain fracture toughness of 300M steel. Sample thickness—0.0127 m (0.5 in.); long-transverse orientation; single data points.

## Microscopy

**Structure and Substructure.** The austenitic grain size progressively increased with austenitizing temperature as indicated in Table I. Optical metallography also revealed that the martensitic plate size increased with increasing austenitic grain size. Electron microscopy of the as-quenched specimens revealed four significant features: a) All Class A specimens but no Class B specimens contained evenly distributed undissolved particles. b) The martensitic substructure in all specimens consisted of laths and plates, and very few of the plates exhibited midrib twinning. c) Auto-tempering was prevalent in the martensitic substructure. d) Untransformed austenite was found at the lath and plate boundaries. These structural features shall be discussed in order.

The undissolved particles, observed only in Class A specimens, varied in size with diameters ranging from 1000 to 2000Å. Their structure was identified by electron diffraction as fcc with lattice parameter of 10.5Å. Figure 5 is a bright field image of a Class A specimen in the untempered condition showing these undissolved particles. They were found inside the laths and plates and also at their boundaries. Specimens austenitized at 1255 K (1800°F) and above did not contain such particles.

Table I. Effect of Austenitizing Treatment on Austenitic Grain Size

Austenitizing Temperature, K (°F)	1144 (1600)	1255 (1800)	1366 (2000)	1477 (2200)
ASTM Grain Size	8	5	3½	1

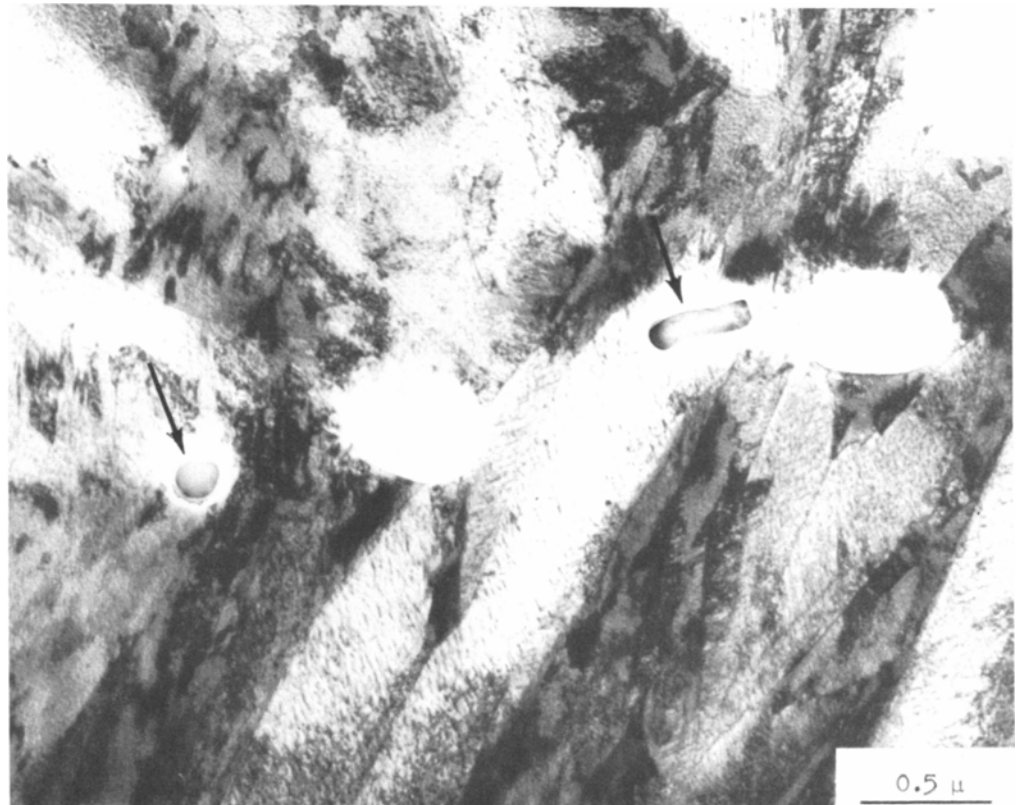
In all the as-quenched samples the martensitic substructure consisted mainly of plates and laths and very few partially twinned plates. The morphological classifications of martensite have already been established by previous workers<sup>8,28,29</sup> and need no amplification here. The extent of twinning was low (less than 5 pct of the martensitic plates were twinned) in both Classes A and B specimens. The dissolution of the above particles in Class B specimens was not accompanied by any observable change in martensitic substructure.

Auto-tempering was extensive in Classes A and B specimens and almost every plate and lath exhibited auto-tempered  $\epsilon$ -carbides. They were very fine and may be seen in Fig. 6.

The presence of retained austenite in the as-quenched martensite has been reported by earlier workers.<sup>30,31</sup> In the present study this retained austenite occurred in such low amounts that conventional X-ray diffraction techniques barely revealed its presence. The austenite, in most cases, outlined the lath and plate boundaries and in some instances occurred in thin platelets. Figure 7 shows bright and dark field images of a specimen quenched from 1144 K (1600°F). It was found by extensive observation that the extent of the interlath and plate austenite was quite comparable in Classes A and B specimens, and no significant differences in the quantity of retained austenite could be detected.

Tempering of the steel produced analogous changes in microstructure in Class A and Class B specimens. All the specimens tempered at 477 K (400°F) and 589 K (600°F) contained  $\epsilon$ -carbide precipitates that were coarser than the size observed in the as-quenched structure. Retained austenite was still

Fig. 5—300M steel specimen austenitized at 1144 K (1600°F) and quenched to room temperature. Bright field image showing the presence of undissolved particles (indicated by arrows).



present at the boundaries and could be readily observed in the structure. Tempering at 700 K (800°F) partially spheroidized the cementite particles. Retained austenite at the lath boundaries decomposed to cementite and, presumably, ferrite leaving a network of lath boundary carbides. Figure 8 shows the bright and dark field images of a Class A specimen tempered at 700 K (800°F) showing discrete cementite precipitates at the lath boundaries. Isolated instances of retained austenite could also be found.

Tempering at 811 K (1000°F) also spheroidized the cementite, and those spheroids were observed in the matrix and the boundaries as shown in Fig. 9. The retained austenite was totally absent.

**Fractography.** Figure 10 shows a series of fractographs of the tested fracture toughness specimens quenched from 1144, 1255, and 1477 K (1600, 1800, and 2200°F). The fracture morphology is radically different between Class A and Class B specimens. Class A specimens showed a mixture of quasicleavage and dimpled rupture in proportions depending on the tempering temperature. No intergranular failure was observed at any tempering temperature. Class B specimens also failed by a mixture of quasicleavage and dimpled rupture in the tempering range of 477 to 589 K (400 to 600°F) but with somewhat less quasicleavage than Class A specimens. In sharp contrast tempering at and above 700 K (800°F) caused the Class B specimens to fail by an intergranular mode. In each case, the fractographs were compared with the optical micrographs to verify that intergranular failure was indeed along the prior austenite grain boundaries.

A limited number of high resolution fractographs were prepared by gold coating the fracture surfaces in an attempt to locate the particles which had been

observed in Class A samples by transmission electron microscopy. Particles of the proper size were found concentrated only on the quasicleavage regions of Class A specimens, a typical example of which is shown in Fig. 11. Smaller (500Å) particles were found localized on the quasicleavage fracture region of specimens tempered at 1200 K (1700°F) and at 1255 K (1800°F). However, only one quasicleavage region was observed in the latter specimen.

## DISCUSSION

### Significant Observations

The most significant observations from the present research are the following:

A) Tempering in the range of 477 to 589 K (400 to 600°F) produced substantially higher toughness in Class B specimens than in Class A specimens. On the other hand, tempering at 700 to 811 K (800 to 1000°F) reversed the above trend. Tempering at 700 K (800°F) produced a minimum in the toughness *vs* tempering temperature curves for Class B specimens.

B) The microstructure of both classes as determined by transmission electron microscopy was qualitatively alike. After tempering at temperatures below 700 K (800°F) the structure consisted of a uniform dispersion of  $\epsilon$ -carbide in lightly twinned martensite with small amounts of austenite in the lath and plate boundaries. After tempering at or above 700 K (800°F) the  $\epsilon$ -carbide transformed to cementite and the retained austenite decomposed to ferrite and cementite. However the following differences were noted between Classes A and B specimens: 1) Class A samples were found to have undissolved particles. These appeared to be completely dissolved in the

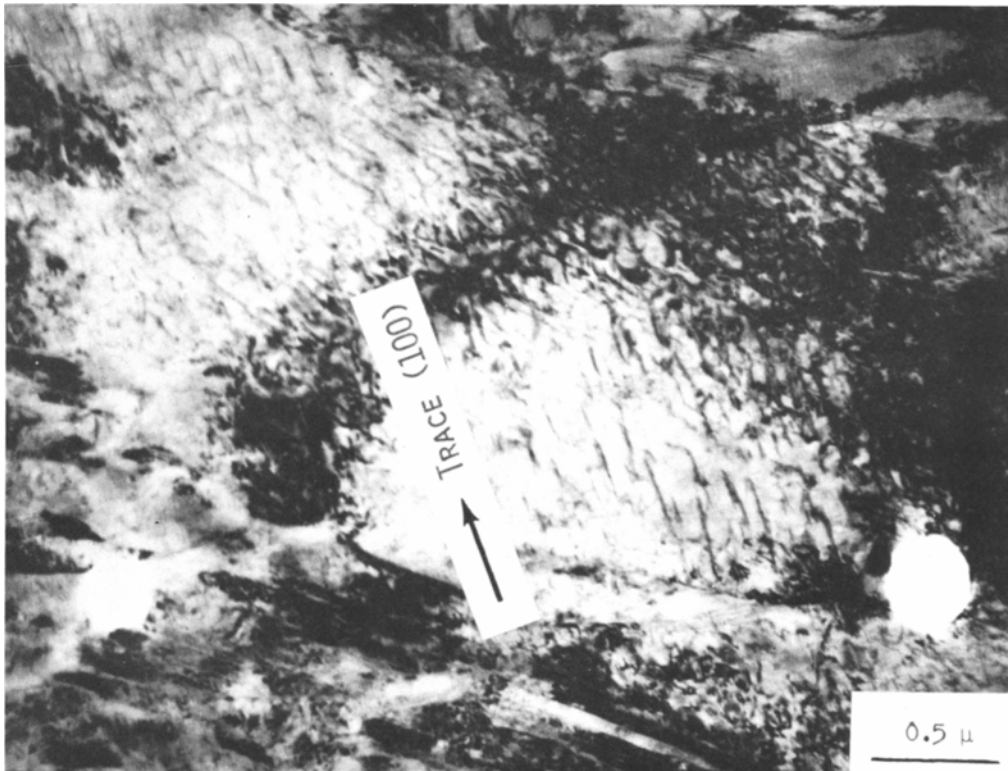
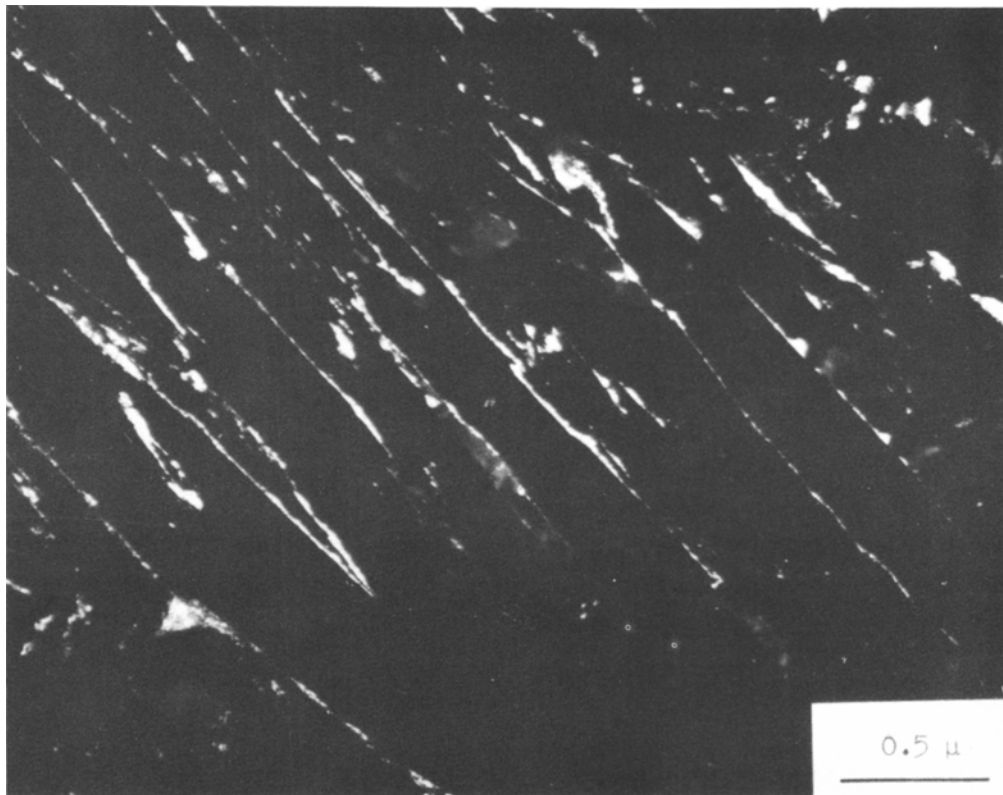


Fig. 6—300M steel specimen austenitized at 1144 K (1600°F) and quenched to room temperature. Bright field image shows auto-tempered  $\epsilon$ -carbide in a martensitic plate.



Fig. 7—300M steel specimen austenitized and quenched from 1144 K (1600° F). Bright field image (top) shows martensitic substructure. Autotempering is evident in the laths. The dark field image of a (200)  $\gamma$  reflection (bottom) reverses the contrast of the austenite at the interlath boundaries. An undissolved particle is indicated by an arrow in the top photograph.



Class B specimens. 2) The quasicleavage regions of fracture surfaces of Class A samples contained high concentrations of particles similar in appearance and size to the above undissolved particles.

C) Fracture surfaces were transgranular except for Class B specimens tempered at or above 700 K (800°F). These failed by intergranular cleavage.

#### As-Quenched Structure

Some recent studies<sup>32,33</sup> indicate that use of a higher austenitizing temperature followed by oil quenching

but no subsequent tempering provides high toughness in some commercial steels. The present work cannot confirm these results for 300M steel. Optical and transmission electron microscopy results have shown that the as-quenched structure is uniformly martensitic with small amounts of austenite at the lath and plate boundaries. Since all the as-quenched fracture specimens showed transgranular failure, it follows that austenite at the lath and plate boundaries does not mitigate brittle failure in the as-quenched condition. The transgranular nature of the as-quenched fracture toughness specimen also rules out any possibility of

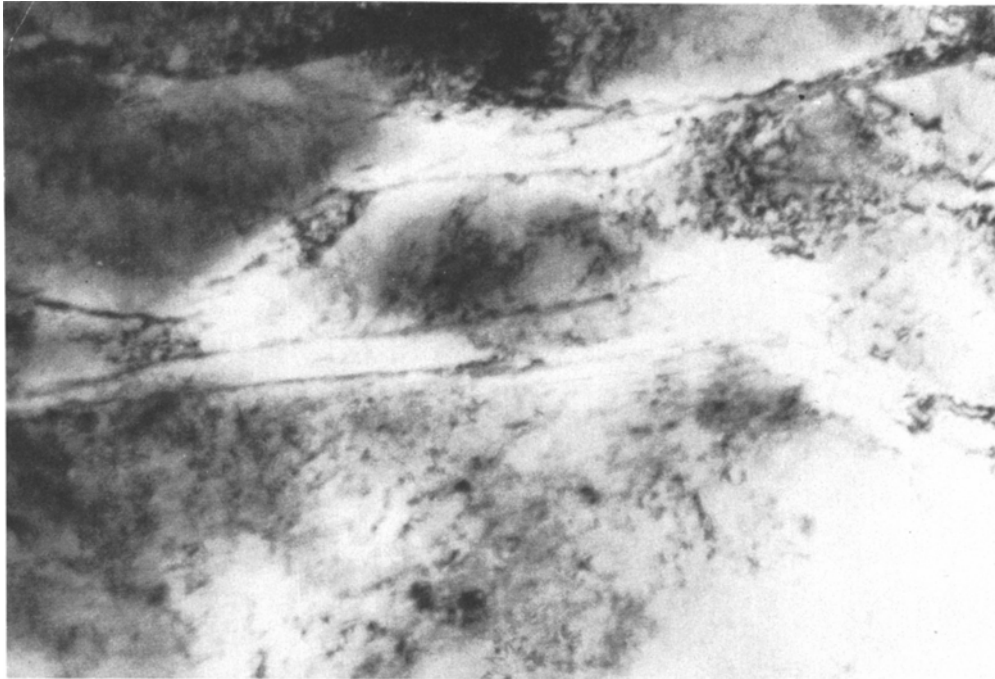
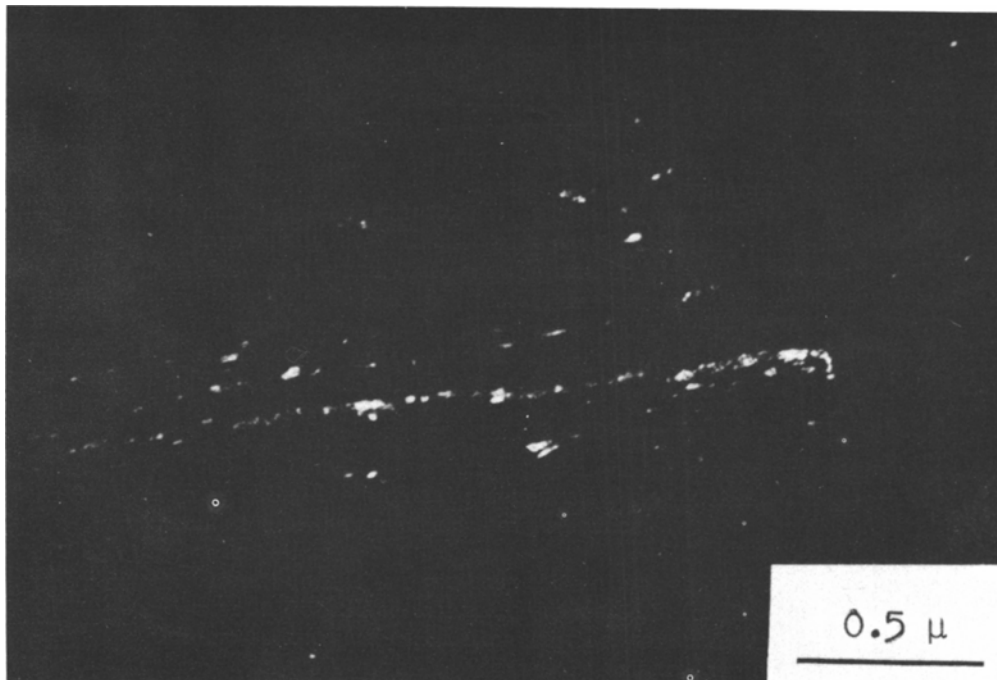


Fig. 8—300M steel specimen austenitized and quenched from 1144 K (1600°F) and double tempered at 700 K (800°F). Bright field image shows martensitic substructure. Precipitation of cementite is not obvious in the bright field image, but the imaging of a cementite reflection (bottom) reveals cementite precipitates in the dark field image.



impurity segregation at the grain boundaries as suggested by McMahon<sup>34</sup> who observed intergranular failure in as-quenched specimens. Thus the austenite grain size has no significant effect on the toughness of the as-quenched steel.

#### Quenched and Tempered Structures

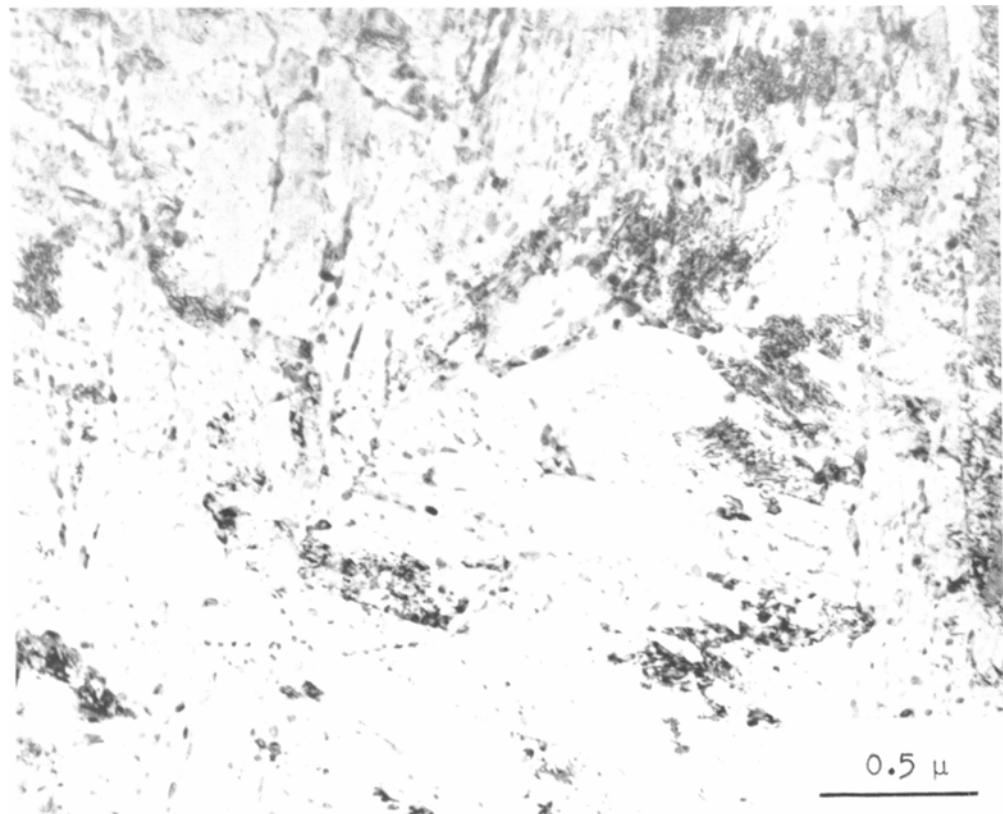
Tempering Temperature Below 700 K (800°F). The effect on toughness of microstructural changes accompanying austenitizing temperatures can be evaluated from Table I and Figs. 1 and 4. Increase of austenitizing temperature caused an increase in austenitic grain size and, between 1144 K (1600°F) and 1255 K (1800°F) resulted in dissolution of the second phase particles discussed above. Specimens tempered at 477 K (400°F) and 589 K (600°F) experienced increases in toughness with austenitizing temperature with the most pronounced improvement occurring concurrently with the dissolution of the second phase particles. Thus it appears possible that the second phase particles facilitated crack propagation in the tempered Class A specimens, and their removal resulted in higher toughness. Improvement in toughness with increasing austenite grain size has been noted earlier,<sup>32,33</sup> and some of the increase in toughness with increasing austenitizing temperature can be attributed to this effect. As-quenched toughness is relatively unaffected by austenitizing temperature.

The present results show that twins in martensite are not sufficient to cause low toughness. Both Class A and Class B specimens possess comparable but low amounts of twins and the toughness responses are widely different. The structure which produced

the highest toughness values consisted of uniform  $\epsilon$ -carbide precipitates in a martensitic matrix. Reports by Lindborg and Averbach<sup>35</sup> and Liu<sup>16</sup> showed that coherency strain associated with  $\epsilon$ -carbide is fairly isotropic and hence does not retard the crack growth as much as the cementite precipitate does in a bainitic structure. The present results show that the toughness of the martensitic structure with  $\epsilon$ -carbide precipitates is high in the absence of undissolved precipitate particles. The question that still remains unanswered relates to the brittleness of the untempered martensitic structure. The as-quenched microstructure consisted of a fine dispersion of auto-tempered  $\epsilon$ -carbide in a martensitic matrix. Tempering at 477 K (400°F) only caused the  $\epsilon$ -carbide precipitates to grow, but the toughness of the steel improved appreciably. It can be speculated that the  $\epsilon$ -carbide formed during quenching depletes the carbon locally and thus renders the carbide/matrix interface weak.

Tempering Temperatures of 700 K (800°F) and Above. The low toughness of Class B specimens after tempering at 700 K (800°F) or higher can possibly be explained in the same manner as "350°C embrittlement",<sup>34,36-38</sup> The observed decohesion along prior austenite grain boundaries clearly suggests that the micromechanism(s) propagating the failure is definitely at the grain boundary rather than in the matrix. It has been reported<sup>37,39</sup> that the severity of embrittlement is accentuated by large austenitic grains which is in accordance with the present results. The steel used in the present investigation has a lower phosphorous content than steels employed earlier,<sup>36,39</sup> and the Class A specimens with

Fig. 9—300M steel specimen austenitized at 1477 K (2200°F) and double tempered at 811 K (1000°F). Bright field image shows spheroidized cementite precipitates at the lath and plate boundaries.



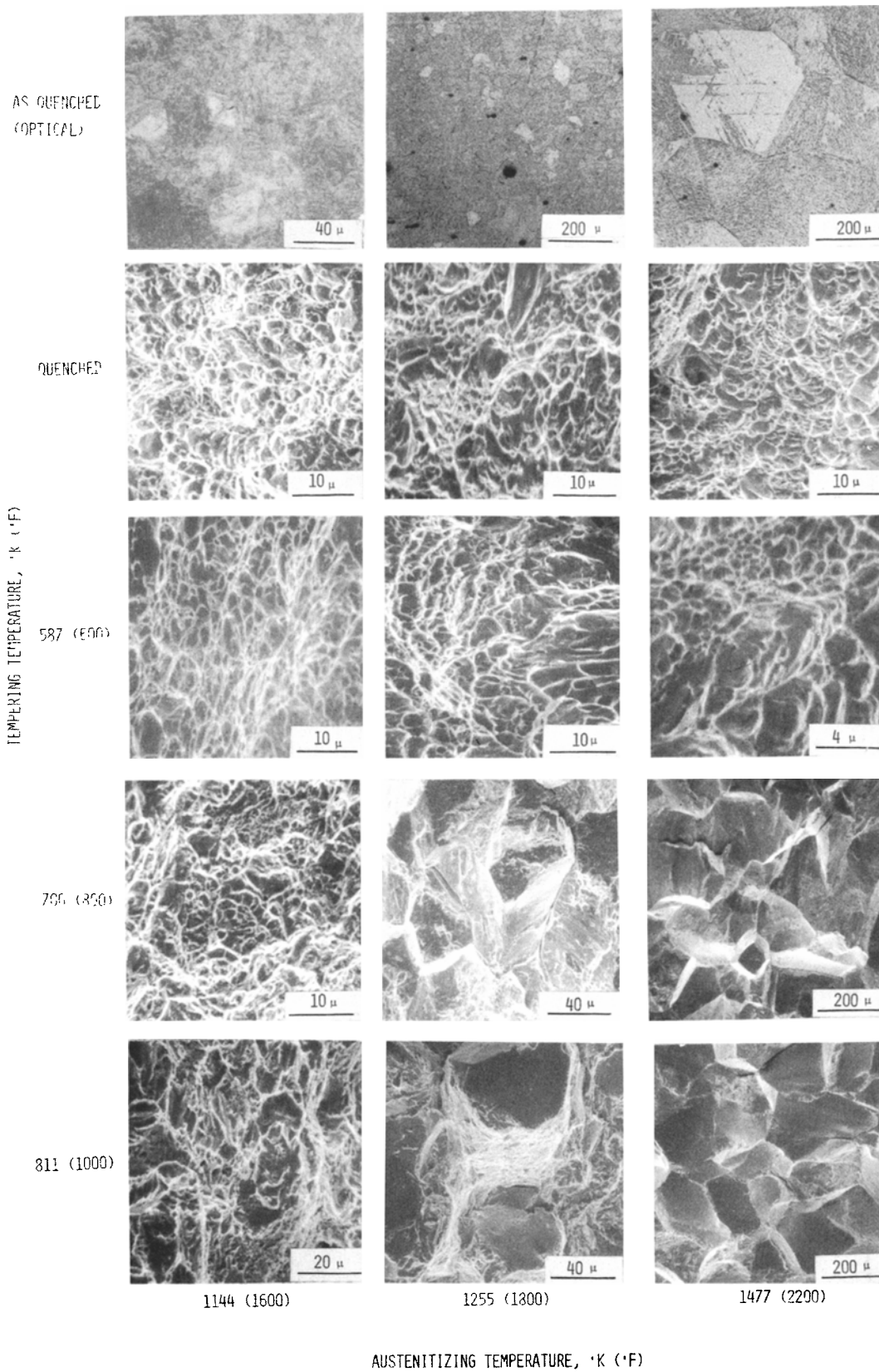


Fig. 10—Series of optical micrographs and scanning fractographs illustrating the fracture morphology of heat treated and tested fracture toughness specimens. Optical micrographs are included for grain size reference.



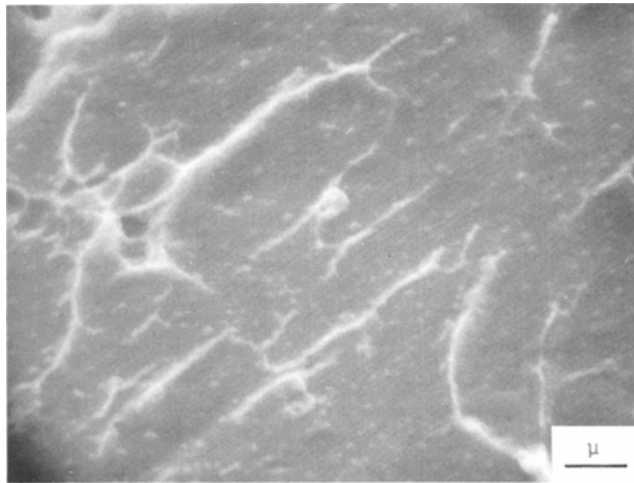
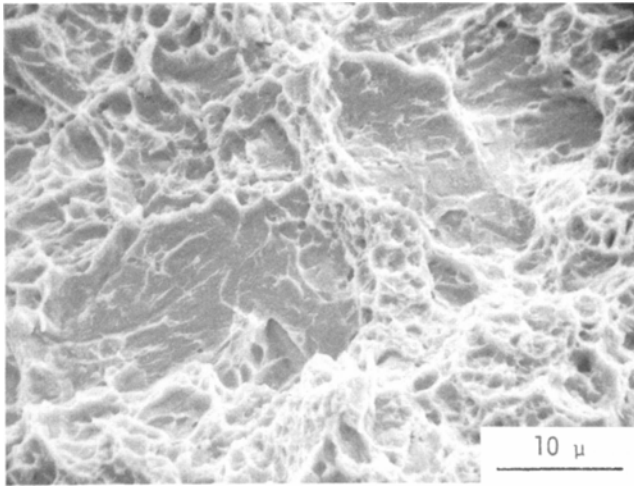


Fig. 11—High resolution fractograph showing concentration of undissolved particles on quasi-cleavage region of the fracture surface of a Class A specimen austenitized at 1144 K (1600°F) and double tempered at 587 K (600°F).

austenite grain size 8 were practically free from this embrittlement. Similar observations were made by Woodfine.<sup>39</sup> It thus appears that a cutoff grain size for embrittlement exists in 300M steel somewhere between ASTM grain sizes 5 and 8.

#### SUPPLEMENTARY EXPERIMENTS

Because the second phase particles which seemed responsible for reducing toughness in the Class A heat treatments appeared to be completely dissolved after 1 h at 1255 K (1800°F), additional studies were performed in the austenitizing region between the Class A and the Class B treatments. Samples were austenitized at a variety of times and temperatures and examined by TEM to determine the lowest austenitizing temperature which would dissolve the particles. Austenitizing times up to 8 h at 1144 K (1600°F) did not dissolve the particles, nor did 1 h at 1172 K (1650°F). However, 1 h at 1200 K (1700°F) eliminated most of the precipitates, and this time and temperature were selected for supplementary plane strain fracture toughness determinations.  $K_{IC}$  was evaluated as before using the 0.0127 m (0.5 in.) sam-

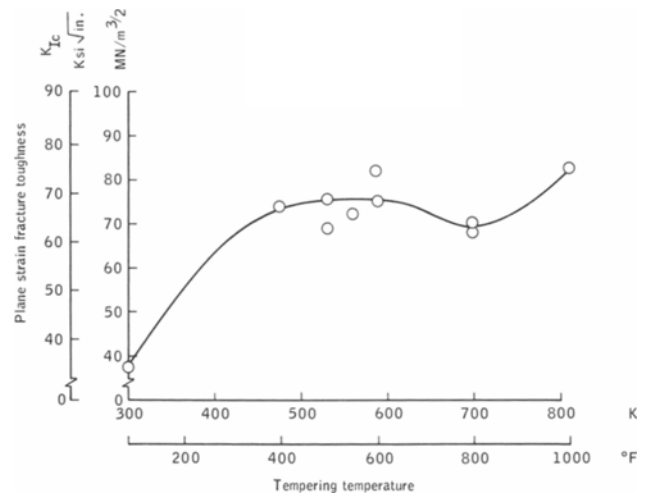


Fig. 12—Effect of tempering temperature on plane-strain fracture toughness of 300M steel austenitized at 1200 K (1700°F). Long transverse orientation and single data points used.

ple thickness. The results are shown in Fig. 12 where it can be seen that this heat treatment resulted in behavior which was intermediate between Class A and Class B material. The data scatter was greater than expected, and no reason could be found to explain it from either the test procedures or the heat treatment.

#### SUMMARY

Improvement in fracture toughness of 300M steel can be effected by austenitizing at higher temperatures than the conventionally used temperature of 1144 K (1600°F). This enhancement in toughness was attributed to dissolution of second phase particles.

For optimum strength and toughness it is recommended that the steel be austenitized at 1255 K (1800°F) and tempered in the range 477 K (400°F) to 589 K (600°F).

Retained austenite was observed at the lath and plate boundaries in all the specimens tempered at 589 K (600°F) and below. This austenite decomposed to ferrite and cementite on tempering at 700 K (800°F) and above.

Tempering at 700 K (800°F) and above caused intergranular embrittlement in specimens austenitized at and above 1255 K (1800°F).

#### ACKNOWLEDGMENTS

The heat treatments were performed by Advanced Technology Center, Inc., Dallas, Texas, under the direction of Dr. Roger D. Goolsby. Dr. Raghavan's contributions to this research were made possible through a NAS/NRC Postdoctoral Resident Research Associateship.

#### REFERENCES

- 1 D. Huang and G. Thomas: *Met. Trans.*, 1972, vol. 2, p. 1587.
- 2 V. F. Zackay, E. R. Parker, R. D. Goolsby, and W. E. Wood: *Nature Phys. Sci.*, 1972, vol. 236, no. 68, p. 108.

3. S. K. Das and C. Thomas: *Trans. ASM*, 1969, vol. 62, p. 659.
4. G. Thomas, D. Schmatz, and W. W. Gerberich: *High Strength Materials*, V. F. Zackay, ed., p. 199, J. Wiley and Sons, New York, N.Y., 1965.
5. B. R. Banerjee. *J. Iron Steel Inst.*, 1965, vol. 203, p. 166.
6. A. J. Baker, E. J. Lauta, and R. P. Wei: *Structure and Properties of Ultra High Strength Steels*, ASTM STP 370, p. 3, ASTM, Philadelphia, Pa., 1965.
7. E. W. Page, P. Manganon, Jr., G. Thomas, and V. F. Zackay *Trans ASM*, 1969, vol. 62, p. 45.
8. P. M. Kelly and J. Nutting: *Physical Properties of Martensite and Bainite*, ISI Spec. Rep. 93, Iron and Steel Institute, London, 1965.
9. John R. Low, Jr.: *Eng. Fract. Mech.*, 1969, vol. 1, p. 55.
10. G. E. Pellissier: *Eng. Fract. Mech.*, 1968, vol. 1, p. 55.
11. Lew F. Porter: *Seminar on Fracture Control, Theory, and Applications*, Philadelphia, Pa., 1970.
12. B. R. Banerjee: *Structure and Properties of Ultra High Strength Steels*, ASTM STP 370, p. 94, ASTM, Philadelphia, Pa., 1968.
13. G. T. Hahn and A. R. Rosenfield: *Applications Related Phenomena in Titanium and its Alloys*, ASTM STP 432, p. 5, ASTM, Philadelphia, Pa., 1968.
14. Y. H. Liu: *Trans ASM*, 1969, vol. 62, p. 55.
15. C. Vishnevsky and E. A. Steigerwald. *Trans ASM*, 1965, vol. 62, p. 305.
16. Y. H. Liu. *Trans. ASM*, 1969, vol. 62, p. 544.
17. E. B. Kula and A. A. Anctil *J. Mater.*, 1969, vol. 4, no. 4, p. 817.
18. B. S. Lement, B. L. Averbach, and Morris Cohen: *Trans. ASM*, 1954, vol. 46, p. 851.
19. J. S. Pascover and S. J. Matas: *Structure and Properties of Ultra-High Strength Steels*, ASTM STP No. 370, p. 30, ASTM, 1965.
20. L. J. Klingler, W. J. Barnett, R. P. Frohberg, and A. R. Troiano: *Trans. ASM*, 1954, vol. 46, p. 1557.
21. R. O. Ritchie, B. Francis, and W. L. Server: *Met. Trans A*, 1976, vol. 7A, p. 831.
22. S. L. Pendelberry, R. F. Simenz, and E. K. Walker. *Fracture Toughness and Crack Propagation of 300M Steel*, Report No. DS-68-18, Lockheed-California Company for Department of Transportation, Federal Aviation Administration, 1968.
23. J. H. Bucher, G. W. Powell, and J. W. Spretnak: *Application of Fracture Toughness Parameters to Structural Metals*, Herman D. Greenberg, ed., p. 323, Gordon and Breach, New York, N.Y., 1966.
24. W. E. Wood, E. R. Parker, and V. F. Zackay: Rept. No. LBL-1474, May, 1973.
25. W. E. Wood: *Eng. Fract. Mech.*, 1975, vol. 7, p. 219.
26. J. L. Youngblood: *Trans. ASM*, 1969, vol. 62, p. 1019.
27. J. L. Youngblood and M. Raghavan. *AIAA/ASME/SAE 16th Structures, Structural Dynamics and Materials Conference*, Denver, May, 1975.
28. G. Thomas. *Met. Trans.*, 1971, vol. 2, p. 2373.
29. P. M. Kelley and J. Nutting: *J. Iron Steel Inst.*, 1961, vol. 197, p. 199.
30. J. A. McMahon and G. Thomas: *Proc. Third Intl. Conf. on the Strength of Metals and Alloys*, vol. 1, p. 180, Institute of Metals/Iron and Steel Institute, Cambridge, England, Aug., 1973.
31. G. Y. Lai, W. E. Wood, R. A. Clark, V. F. Zackay, and E. R. Parker: *Met. Trans.*, 1974, vol. 5, p. 1663.
32. W. E. Wood: Ph.D. Thesis, University of California, 1972.
33. R. O. Ritchie and J. F. Knott: *Met. Trans.*, 1974, vol. 5, p. 782.
34. C. J. McMahon, Jr.: *Temper Embrittlement—An Interpretive Review*, ASTM STP 407, ASTM, Philadelphia, Pa., 1969.
35. V. H. Lindborg and B. L. Averbach: *Acta Met.*, 1966, vol. 14, p. 1590.
36. J. M. Capus and G. Mayer: *Metallurgica*, 1960, vol. 62, p. 133.
37. J. M. Capus: *J. Iron Steel Inst.*, 1962, vol. 200, p. 922.
38. J. M. Capus: *The Mechanism of Temper Brittleness*, ASTM STP 407, ASTM, Philadelphia, Pa., 1969.
39. B. C. Woodfine: *J. Iron Steel Inst.*, 1953, vol. 173, p. 229.